



Wear behavior and machining quality of novel high-sharp brazed diamond abrasive core drills during drilling SiC_f/SiC composite micro-holes

Jingyuan He¹ · Ning Qian^{1,2} · Honghua Su¹ · Yucan Fu¹ · Wenfeng Ding¹ · Jiuhua Xu¹

Received: 4 March 2023 / Accepted: 10 August 2023 / Published online: 23 August 2023
© The Author(s), under exclusive licence to Springer-Verlag London Ltd., part of Springer Nature 2023

Abstract

SiC_f/SiC composites have promising applications in aerospace industries. SiC_f/SiC composite micro-holes are important components, such as gas film holes on turbine blades. However, micro-hole machining in the SiC_f/SiC composite is challenging because of its excellent mechanical and physical properties and poor machinability caused by micro-hole constraints. Therefore, a novel brazed diamond abrasive core drill was designed to achieve high self-sharpness by continuously losing blunt diamond grits and exposing sharp diamond grits. The wear and self-sharpness of the developed drill were investigated and compared with those of an electroplated diamond core drill during ultrasonic vibration-assisted drilling of SiC_f/SiC composite micro-holes. The material removal behaviors of SiC_f/SiC composites, including drilling forces, exit tearing, hole dimensions, hole wall quality, and the wear of core drills, were also studied. The developed core drill demonstrated reduced drilling force and a significantly prolonged lifetime. Further, it achieved superior drilling performance, drilling accuracy, and micro-hole quality.

Keywords SiC_f/SiC composite · Micro-hole · Brazed diamond abrasive core drill · Self-sharpness · Lifetime

1 Introduction

Silicon carbide fiber-reinforced silicon carbide ceramic matrix composites (SiC_f/SiC composites) have attracted wide attention in power, aerospace, and other industries because of their excellent properties, such as high-temperature resistance, high specific strength, corrosion resistance, and wear resistance [1–4]. In these industries, the SiC_f/SiC composites have been used in manufacturing some key components, which generally contain many difficult-to-machine structures, such as micro-holes (diameter usually smaller than 1.5 mm) [5, 6]. For example, SiC_f/SiC composite blades of a gas turbine in power plants contain hundreds

of micro-holes [7, 8]. Despite the excellent physical and mechanical properties of SiC_f/SiC composites, the constraints governing the machining of a micro-hole structure cause rapid wear of the drilling tool, which may even fail to drill one SiC_f/SiC composite micro-hole in its lifetime [9–12]. Therefore, machining good-quality SiC_f/SiC composite micro-holes is extremely challenging.

Presently, the methods of machining SiC_f/SiC composite micro-holes mainly include mechanical drilling, laser-assisted machining [13–15], and water jet machining [16–18]. Laser-assisted machining is a non-contact machining method that does not involve the problem of tool wear [19]. This has great advantages in the field of small-hole machining. However, laser-assisted machining inevitably produces a heat-affected layer, which significantly affects the mechanical properties of the SiC_f/SiC composite [20]. With the increase in the drilling depth, the shift in the laser focus makes it difficult to guarantee drilling accuracy, and a drum-shaped hole may be machined [21]. Therefore, this machining method has certain limitations in deep and small-hole machining [22]. In addition, the SiC_f/SiC composite contains voids, preventing using a liquid coolant in the machining process. Without a coolant, the liquid remaining in the SiC_f/SiC composite

✉ Ning Qian
n.qian@nuaa.edu.cn

✉ Honghua Su
shh@nuaa.edu.cn

¹ Nanjing University of Aeronautics and Astronautics,
Nanjing 210016, China

² JITRI Institute of Precision Manufacturing, Nanjing 211806,
China

easily causes high-temperature oxidation during operation under high-temperature conditions, resulting in fast failure [23]. Therefore, water jets are rarely used to machine SiC_f/SiC composites under these working conditions. Electrical discharge machining (EDM) has also been used to machine holes in SiC_f/SiC composites. EDM has low efficiency and high electrode loss and produces a heat-affected zone, which leads to additional post-processing and higher machining cost [24, 25]. Among the aforementioned machining techniques, mechanical machining is a promising method for achieving high-quality SiC_f/SiC composite micro-holes.

During the mechanical machining of micro-holes, the drilling tool (regardless of whether it is a cemented carbide or the harder polycrystalline diamond (PCD) tool) wears rapidly owing to the high hardness and strength of the SiC_f/SiC composite [26–28]. In addition, the dimension of the micro-hole constrains the diameter of the drilling tool, the drilling speed is very low, the dynamic sharpness of the drilling tool is weak, and the machining ability is limited, resulting in poor drilling quality and rapid tool wear. Thus, the major challenge in mechanical machining is severe tool wear. However, this problem has a straightforward solution—a new drilling tool with high wear resistance and self-sharpness should be designed. In addition, a method to increase the dynamic sharpness should be applied.

During the drilling of SiC_f/SiC composite micro-holes using conventional drilling tools (e.g., high-speed steel based twist drills or cemented carbide drills), the tool material is softer than the SiC_f/SiC composite, and rapid tool wear inevitably occurs. In addition, the rigidity of the tools is insufficient, leading to poor drilling stability [10]. Diamond has extremely high hardness (up to 8000 HV) and excellent thermal conductivity (560 W/m·K), and it is the most promising material for high-performance drilling tools [29]. PCD tools were used to drill the SiC_f/SiC composite, which have the advantages of reducing the thrust force and tool wear, thus improving the tool life [30]. However, it has also been reported that the wear of the cutting edge of PCD tools results in increased drilling force and degraded drilling accuracy [28]. Hence, timely replacement of tools is necessary to ensure high drilling quality. Thus, the wear of PCD tools reduces the machining efficiency and increases the machining cost. A diamond core drill can also be used to drill the SiC_f/SiC composite. The drilling process using the core drill is similar to the grinding, that is, the material is removed using diamond grits. Diamond core drills can provide a higher material removal rate, reduce machining damage, prolong the tool life, and improve surface roughness. Studies have shown that diamond core drills are suitable for drilling SiC_f/SiC composite small holes [31, 32]. By optimizing the tool structure and abrasive layer, the

drilling heat and drilling force on the SiC_f/SiC composite can be reduced, and the machined surface quality and tool life can be improved [33, 34]. However, to date, there have been few studies on the dry drilling of SiC_f/SiC composite micro-holes using a diamond core drill. The tool is typically a monolayer electroplated diamond or brazed diamond abrasive core drill. If the single layer of diamond grits wears out, the tool loses its drilling ability and its lifetime is shortened. Therefore, a novel diamond core drill with high self-sharpness and wear resistance must be designed for dry drilling of SiC_f/SiC composite micro-holes.

Ultrasonic vibration-assisted machining applies ultrasonic vibrations in mechanical machining. Ultrasonic vibration increases the machining trajectories of the cutting edges, decreases the dynamic rake angle of the drilling tool, and adds a peening effect [35–38]. Thus, ultrasonic vibration-assisted machining can significantly increase dynamic sharpness [39]. In the case of SiC_f/SiC composites, ultrasonic vibration-assisted drilling (UVAD) can effectively reduce the machining force, delamination, and tear damage of the composite as well as prolong the lifetime of the tools [32, 40]. In addition, UVAD adopts a contact–separation mode, which reduces the contact area between the tool and the workpiece. Consequently, it facilitates chip removal in the drilling process, effectively reduces the friction force, and reduces the drilling temperature [41, 42]. Simultaneously, UVAD decreases the maximum undeformed cutting thickness of the drilling tool, thus reducing the thrust force and improving the drilling quality, particularly by preventing exit tearing of the SiC_f/SiC composite [31, 43].

To machine high-quality SiC_f/SiC composite micro-holes, a novel brazed diamond abrasive core drill with high self-sharpness ability was developed in this study. An electroplated diamond core drill was used to verify the drilling performance of the developed brazed diamond abrasive core drill. The wear progress of both tools was investigated during the ultrasonic-assisted drilling of SiC_f/SiC composite micro-holes. In particular, the self-sharpness behavior of the developed diamond core drill was extensively studied. In addition, the drilling performance, including the drilling force, micro-hole dimensions, hole wall quality, and quality of the developed brazed diamond abrasive core drill, was evaluated.

The remainder of this paper is organized as follows. Section 2 introduces the material and design of the brazed diamond abrasive core drill. Section 3 presents the wear progress of the developed core drill and that of the electroplated diamond core drill. Section 4 discusses the drilling performance of the diamond tools. Section 5 presents the main conclusions.

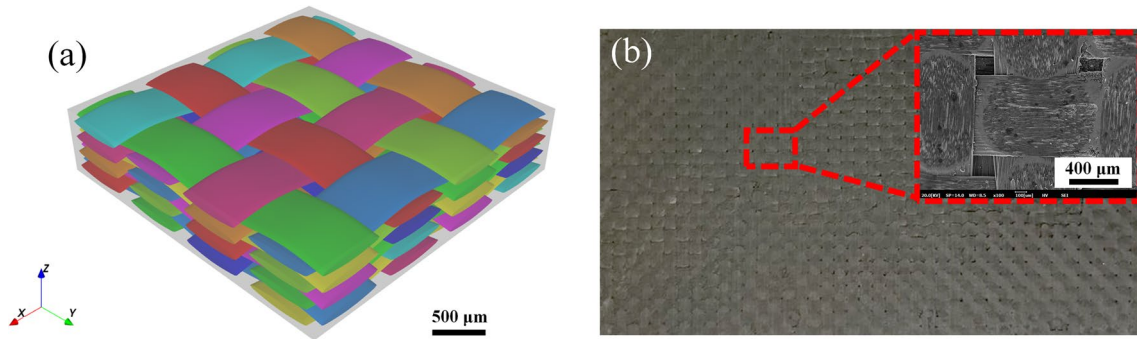


Fig. 1 Structure of 2D SiC_p/SiC composite: **a** schematic of preform structure of SiC fiber and **b** scanning electron microscopy (SEM) image of the cross-sectional observation

Table 1 Mechanical properties of the SiC_p/SiC composite workpiece

Density (g/cm ³)	Elastic modulus (GPa)	Hardness (GPa)	Fracture toughness (MPa·m ^{1/2})
2.29	289	20	26.4

2 Experimental details

2.1 Materials

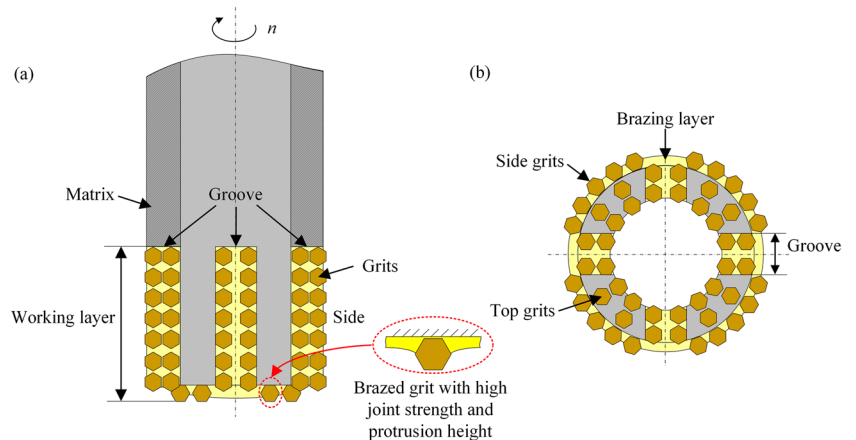
The workpiece was a 2D SiC_p/SiC composite with a thickness of 4 mm. The fiber bundles were orthogonally woven in a plain-weave manner, as shown in Fig. 1a. The material mainly comprised SiC fibers (T300), BN interface layers, a SiC matrix, and pores, as shown in Fig. 1b. The diameter of the SiC fibers was 5–7 μm. The density of the material was 2.0 g/cm³, and the internal porosity was 15–20%. Besides, the surface of the workpiece was coated with a layer of SiC ceramic matrix formed through the CVI (chemical vapor infiltration) process. The SiC ceramic matrix layer enclosed the SiC_p/SiC composite, resulting

in a relatively dense material surface with a low porosity content. The mechanical properties of these materials are listed in Table 1.

2.2 Drilling tools

As mentioned above, the SiC_p/SiC composite has excellent and special mechanical and physical properties. However, the target micro-holes with a diameter of 1.4 mm and the structure can restrict the machining speed, thereby the dynamic sharpness of the core drill. In this study, a novel brazed diamond abrasive core drill with strong self-sharpness ability was designed and fabricated. The novel brazed diamond abrasive core drill has four grooves on the matrix, and several rows of diamond grits are arranged in the grooves (see Fig. 2a). Multiple rows of grits are also arranged on the top of the core drill (see Fig. 2b) and randomly distributed on the side of the core drill matrix. Wear of the core drill, including the grits and matrix on the top, occurs when machining the micro-holes. When the exposed diamond grits are worn out, the diamond grits in the grooves protrude to maintain good sharpness and machinability.

Fig. 2 Schematic of designed brazed diamond core drill: **a** cross-sectional view and **b** top view



Thus, the core drill achieves excellent self-sharpness for drilling micro-holes and has a long lifetime.

For comparison, an electroplated diamond core drill, which is commonly used in research and industry, was also fabricated and analyzed. Single-layer diamond grits were electroplated on the top and side of the core drill matrix, as shown in Fig. 3. It is clear that the working layer of the electroplated diamond core drill contains only one layer of diamond grit, and the grits are mechanically embedded in the plating with a small protrusion height (Fig. 3a). In contrast, the developed novel brazed core drill has a thick working layer (the same dimension as the depth of the grooves), and the grits are chemically brazed on the matrix (Fig. 2a). Hence, it is expected to have better machinability and lifetime than the electroplated diamond core drill.

In this study, to machine micro-holes with a diameter of 1.4 mm, a round matrix made of 022Cr17Ni12Mo2 stainless steel, with an outer diameter of 1 mm and inner diameter of 0.5 mm, was used for the brazed diamond abrasive core drill. Four 0.25-mm-wide and 3-mm-deep grooves were

machined on the matrix, and 120-mesh (average diameter of 100 μm) diamond grits were arranged according to the abovementioned method. The diamond grits were brazed on the matrix with Ag–Cu–Ti filler. The fabricated brazed diamond abrasive core drill is illustrated in Fig. 4.

The matrix of the electroplated core drill was also made of 022Cr17Ni12Mo2 stainless steel; the outer and inner diameters of the matrix were 1 and 0.5 mm, respectively. The diamond grit was 120 mesh, and the plating thickness was 0.2 mm. The fabricated electroplated diamond core drill is shown in Fig. 5. The micro-holes of the SiC_p/SiC composite were 4-mm deep; therefore, the length of the work section of the brazed and electroplated diamond core drills was 5 mm.

The dynamic strength of the novel brazed diamond abrasive core drill was tested through simulation to evaluate the tool deformation during micro-hole machining. The mechanical properties of the tool are shown in Table 2 [44]. The brazed diamond abrasive core drill was designed for spindle speeds up to 20,000 rev/min, and in the pre-test,

Fig. 3 Schematic of electroplated diamond core drill: **a** cross-sectional view and **b** top view

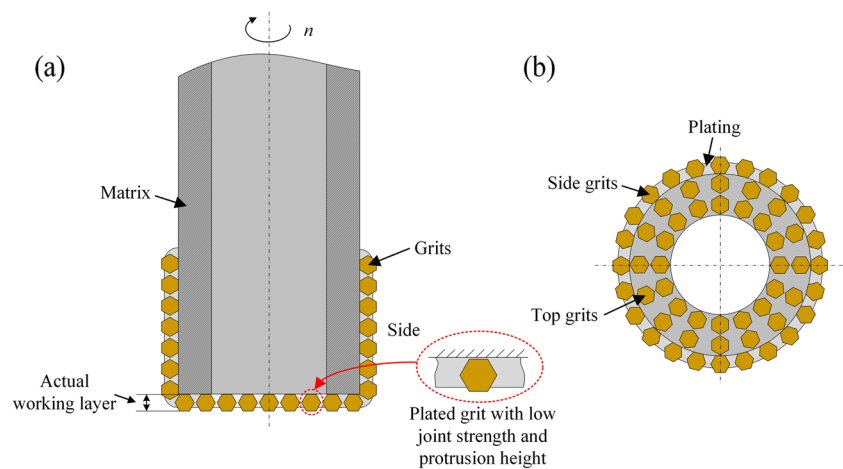


Fig. 4 Fabricated brazed diamond abrasive core drill: **a** picture and SEM photos of **b** top view and **c** side view of the working layer

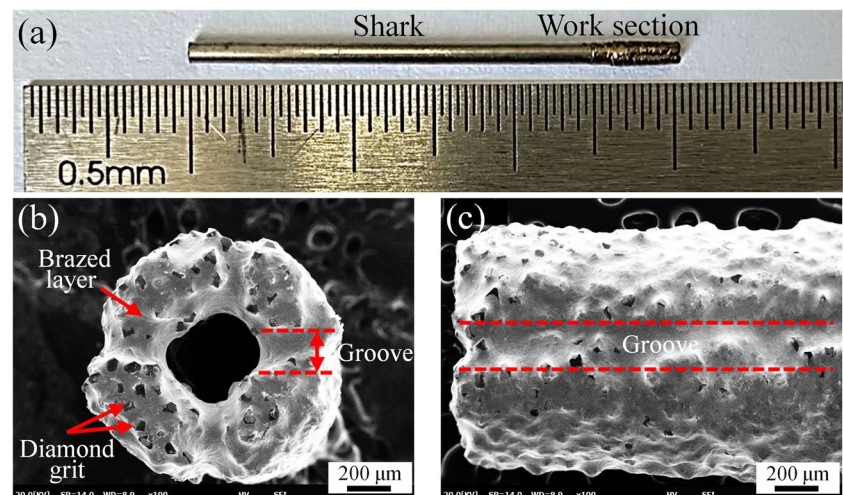


Fig. 5 Electroplated diamond core drill: **a** picture and SEM photos of **b** top and **c** side views of the working layer

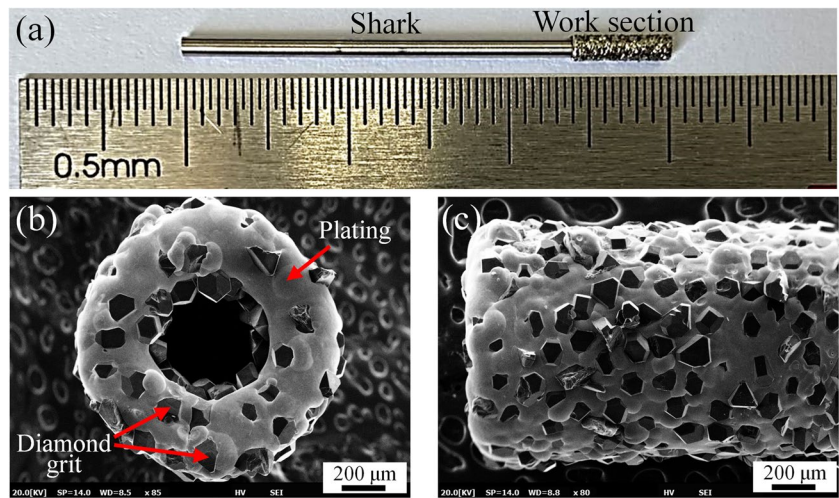


Table 2 Mechanical properties of the tool

Density (g/cm ³)	Young's modulus (GPa)	Poisson's ratio	Yield stress (MPa)
7.95	193	0.28	235

the axial drilling force and torque could reach 10 N and 0.01 N·m, respectively, when drilling the SiC_f/SiC composite micro-holes. The maximum spindle speed, axial force, and torque were loaded onto the designed tool in the simulation, as illustrated in Fig. 6a. The maximum deformation of the designed tool under the above conditions was 1.692 μm, which could be neglected compared to the hole diameter (see Fig. 6b). The maximum equivalent stress was 26.14 MPa, that is, lower than the permissible stress of the matrix material (see Fig. 6c). Thus, the novel brazed

diamond abrasive core drill can be safely used to drill SiC_f/SiC composite micro-holes.

2.3 Experimental setup

The drilling tests were performed on a machining center (DMG Ultrasonic Linear 20). The SiC_f/SiC composite workpiece was mounted on a dynamometer (Kistler 9129AA) by using a fixture. The force signals were then amplified and acquired by an amplifier (Kistler 5080) and DAQ card and processed using DynoWare software. The core drill was held by an ultrasonic tool holder (maximum spindle speed 20,000 rev/min and 30 kHz ultrasonic frequency), as shown in Fig. 7. The diameter and length of the core drill were measured using a tool presetter (EZset 600), as shown in Fig. 8. The tearing of the hole exit and the morphology of the tool wear after drilling are recorded

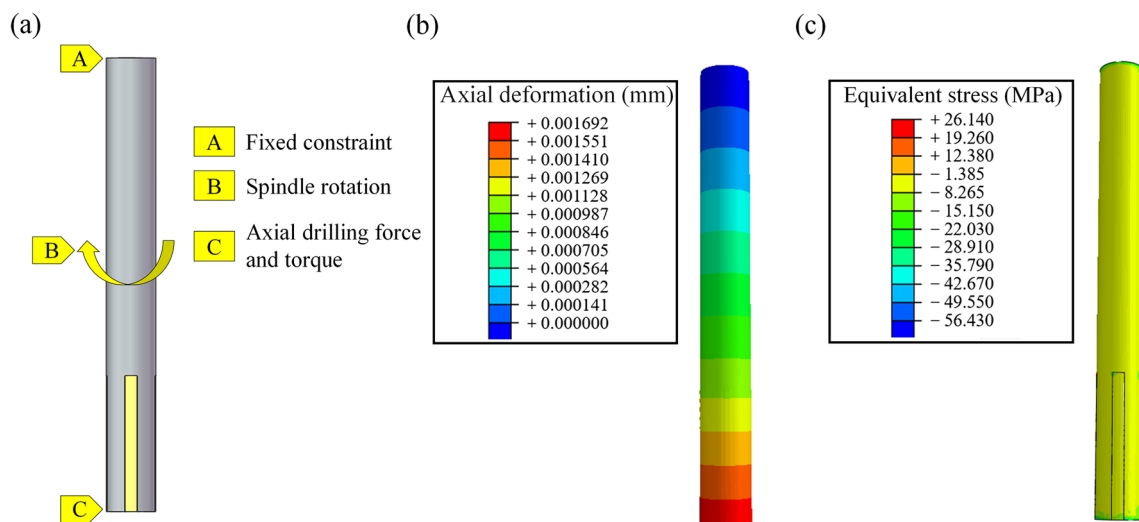


Fig. 6 Dynamic strength of the developed tool: **a** boundary conditions and loads and results of **b** deformation and **c** equivalent stress

Fig. 7 Experimental setup, **a** overall experiment equipment, **b** drilling process, and **c** drilling force measuring device

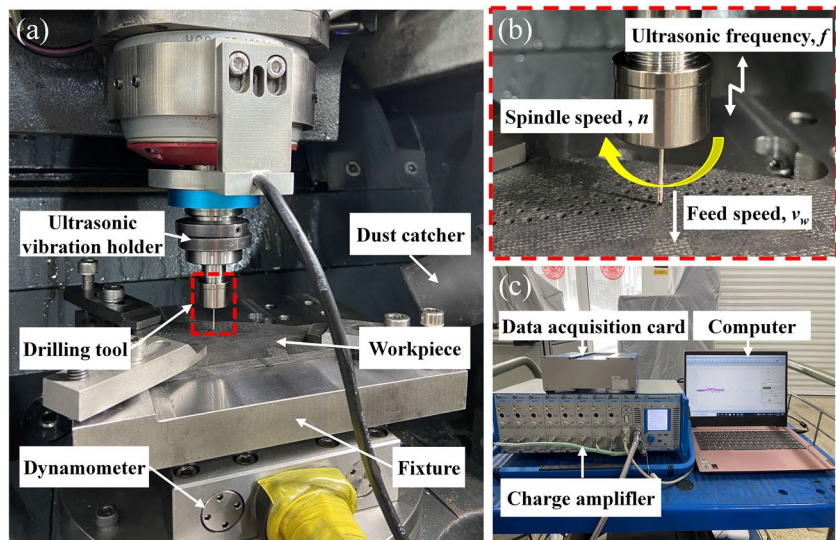
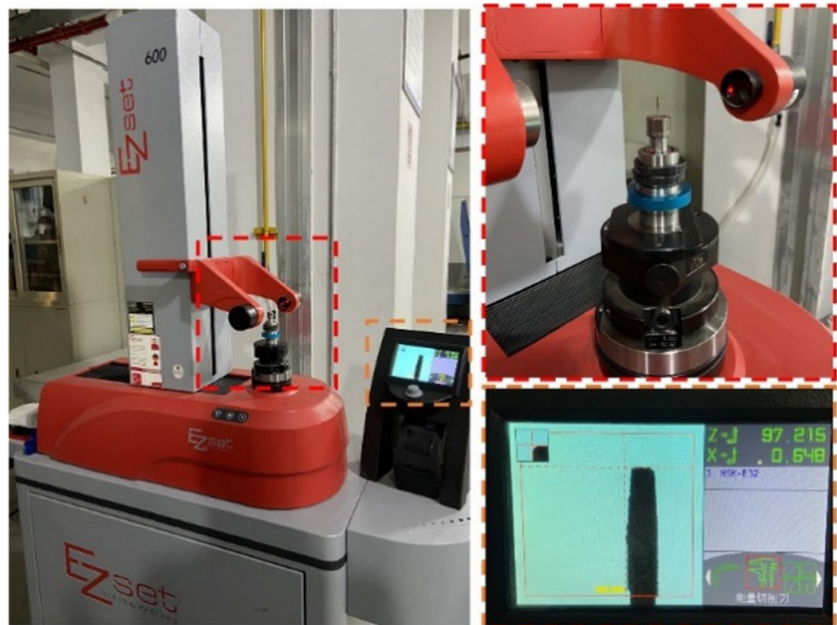


Fig. 8 Core drill dimension measurement



by a 3D video microscope (HIROX KH-7700). Microscopic photos of the self-sharpening behavior of tools are taken by scanning electron microscope (COXEM EM-30 Plus). The confocal microscope (Sensofar Neo S) measures the hole wall's surface roughness S_a , and the results are obtained by measuring each hole three times.

Drilling tests were conducted under dry drilling conditions. To maintain good dynamic machinability, the spindle speed (n) was set to 20,000 rev/min. Based on previous tests, the feed speed (v_w) was set to 1 mm/min. The ultrasonic vibration frequency (f) of the core drill generated by the tool holder was measured as 30.7 kHz, and the amplitudes (A) was 5 μm . The drilling parameters are presented in Table 3.

Table 3 Drilling parameters

Parameter	Value
Spindle speed n (r/min)	20,000
Feed speed v_w (mm/min)	1
Ultrasonic frequency f (kHz)	30.7
Amplitude A (μm)	5
Coolant method	Dry drilling

The diameter and exit tearing factor of SiC_p/SiC composite micro-holes are common indexes to evaluate the drilling quality. The diameter of the micro-holes was measured using a split-ball probe (DIATEST MST-102). Generally, the ratio

of the maximum tearing length to the diameter of the drilling hole is used as the evaluation criterion for the extent of tearing damage around a hole. However, this evaluation criterion is one-dimensional and cannot accurately assess the machining damage of the hole. In this study, a two-dimensional evaluation method that considers the tearing area is employed, and the tearing factor of the hole exit was calculated using Eqs. 1 and 2 [29]:

$$F_D = \frac{A_t}{A_n} \quad (1)$$

$$A_n = \pi R_n^2 \quad (2)$$

where F_D is the tearing factor, R_n is the actual diameter of each drilling hole measured by the split-ball probe (DIAT-EST MST-102), and A_n and A_t are the areas of the micro-hole and exit tearing zone, respectively, as shown in Fig. 9. The measurement of the area of the exit tearing zone A_t is performed using the open-source software ImageJ for image processing and area calculation. First, the captured photograph of the hole exit is subjected to binarization processing (8-bit) using ImageJ. Then, the double threshold image segmentation is applied to segment the region of edge damage in the hole exit, aiming to separate the edge defect area clearly from the background as shown in the yellow region in Fig. 9. And then, use ImageJ's analysis tools, such as "Analyze Particles," to extract defect regions from the image. Finally, the measurement function in the software is employed to calculate the defect area.

3 Tool wear progress

3.1 Tool wear behavior

The novel brazed diamond abrasive core drill with high self-sharpness was then used in the UVAD of SiC_p/SiC

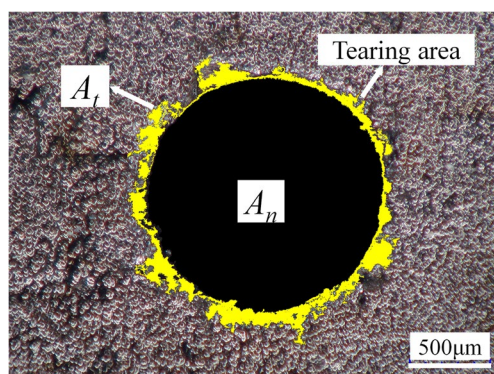


Fig. 9 Exit side of the hole and its tearing area

composite micro-holes. After UVAD of four micro-holes, the brazing layer and some matrix on the top of the core drill were removed along with the grits; subsequently, the grits at the grooves protruded and removed the composite material during the drilling. Eventually, the grits at the grooves showed attrition (white arrows in Fig. 10a). The corner of the core drill started to wear out and some grits at the corner showed attrition, as depicted in Fig. 10b.

After UVAD of eight micro-holes, the brazing layer and matrix were further removed and the grits at the grooves showed macro-fractures; new and sharp grits started to protrude, as shown in Fig. 10c. The worn-out region at the corner expanded (see the green region in Fig. 10d), and attrition and fracture occurred in the grits at the corner, as shown in Fig. 10d.

After UVAD of 20 micro-holes, the brazing layer and matrix of the novel core drill continued to be removed. The grits at the grooves protruded continuously to maintain the sharpness and machinability of the core drill. In addition, some blunt grits fell out, and the grits exhibited attrition and fracture, as shown in Fig. 10e. Along with the removal of the SiC_p/SiC composite, the worn-out region at the corner grew, and the grits at the corner mainly exhibited macro-fractures and fall-outs, as illustrated in Fig. 10f.

Figure 11 shows the diamond grit wear state on the side of the core drill after UVAD of 20 micro-holes. The diamond grits located near the top of the core drill were predominantly characterized by macro-fractures, whereas those situated at the end of the working section exhibited minimal wear, with only a few higher diamond grits displaying macro-fracture. The varying degrees of wear shown by diamond grits in different locations on the core drill can be attributed to the unique drilling characteristics of the brazed diamond abrasive core drill. Specifically, the primary function of the top diamond grits and the side diamond grits near the top of the drill core was to remove the processed materials. These diamond grains were more likely to be worn due to the greater drilling force. On the contrary, the primary function of the diamond grits located at the end of the core drill working section was to establish and maintain precise drilling accuracy while forming the final hole diameter size. During micro-hole drilling, the diamond grits in this section exhibited minimal work-piece material removal, indicating negligible wear of the diamond grit. Additionally, the groove on the side of the drill bit facilitated the efficient removal of chips generated during drilling, thereby minimizing wear on the diamond grits located on the sides of the tool during high-speed rotation. Therefore, the novel brazed diamond abrasive core drill can ensure the number of drilling micro-holes and dimensional accuracy.

Fig. 10 Wear development of the novel brazed diamond abrasive core drill during UVAD: **a**, **b** the wear morphology of the top and side of the core drill for drilling the 4th hole, **c** and **d** drilling the 8th hole, **e** and **f** drilling the 20th hole

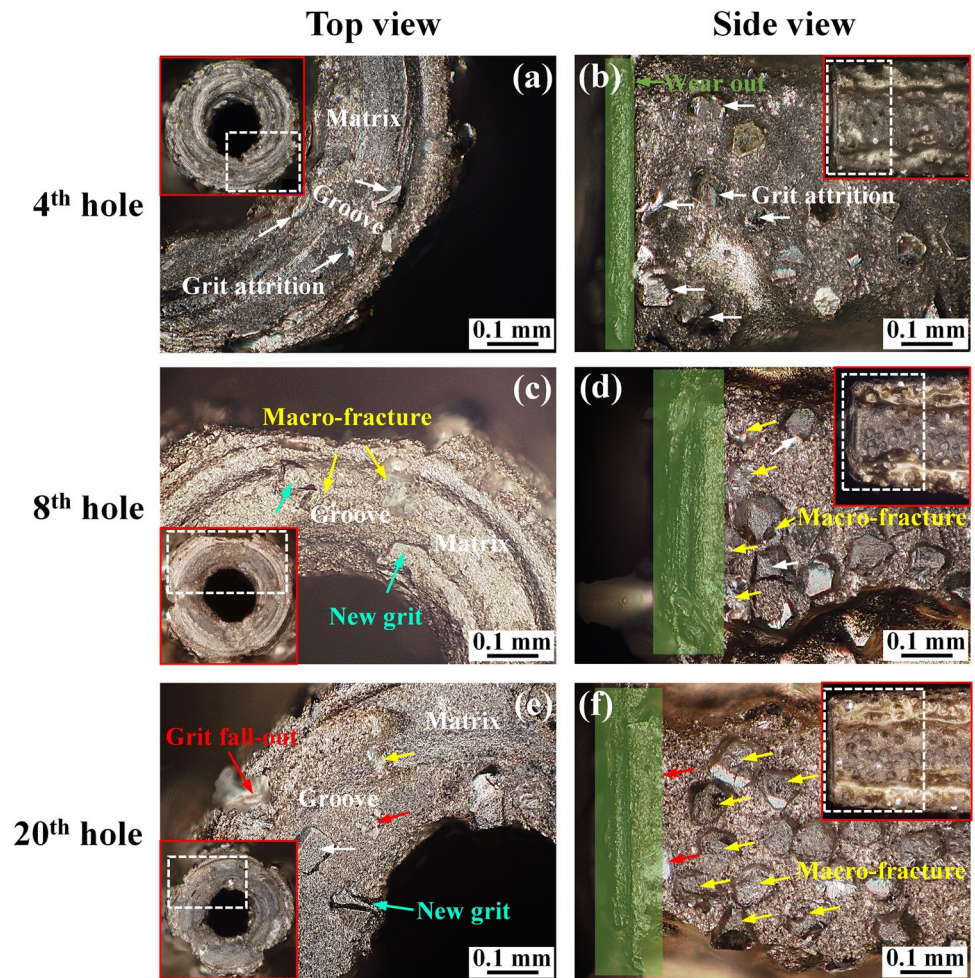


Fig. 11 The diamond grits wear state on the side of the core drill after UVAD of 20 micro-holes: **a** overall of the core drill, **b** the diamond grits near the top of the core drill, and **c** the diamond grits at the end of the core drill

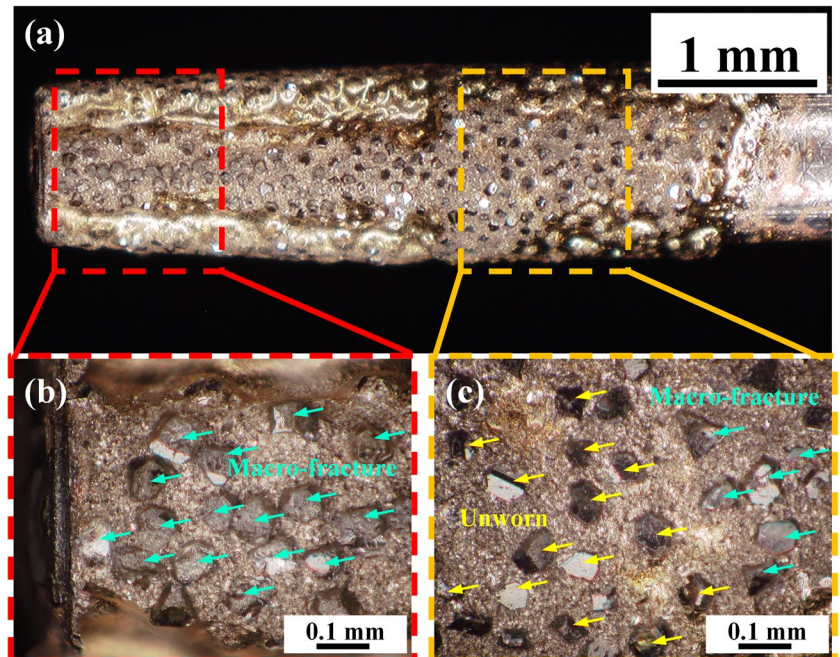
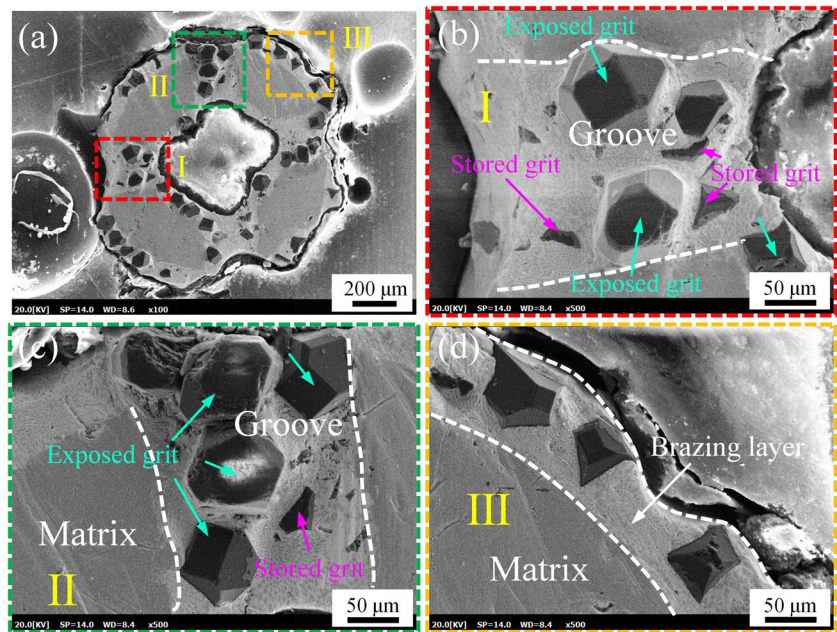


Fig. 12 **a** SEM photo of the top of the brazed diamond abrasive core drill, **b** zoomed photo of section I, **c** zoomed photo of section II, and **d** zoomed photo of section III



3.2 Self-sharpness of the developed tool

After drilling four micro-holes using the developed brazed diamond abrasive core drill, the brazing layer on the top was removed, and the matrix was exposed. In Fig. 12a, the dark gray parts are the matrix, the light gray parts are the brazing layer, and the black parts are the diamond grits. At this stage, the grits on top of the core drill were entirely lost. Along with removing the matrix, the brazing material at the grooves was also removed, and the new and sharp grits at the grooves successfully protruded, as shown in Fig. 12b and c. In addition, some buried grits show only a tip; these will be exposed during the subsequent self-sharpening process (pink arrows in Fig. 12b and c). The grits at the corners also protrude to maintain the sharpness and machinability of the core drill, as shown in Fig. 12d.

During the drilling process, the grits on the core drill suffer attrition, macro-fractures, and even fall-out; the grits become blunt, and the sharpness and machinability of the core drill decrease. As a result, the hard and high-strength SiC_p/SiC composite begins to remove the brazing layer and matrix reversibly; the blunt grits are additionally lost. At this stage, the grits at the grooves begin to protrude, and new and sharp grits restore the sharpness and machinability of the core drill. As the SiC_p/SiC composite is drilled, the grits become blunt again, the brazing layer and matrix are removed, and new grits in the grooves protrude to maintain the sharpness. The entire process is repeated continuously, which forms the self-sharpening process of the developed brazed diamond abrasive core drill, as shown in Fig. 13.

Because the developed core drill loses a part of the brazing layer and matrix during the drilling of each hole, the

length of the core drill reduces gradually. The length reduction (ΔL), when compared with the previous cycle of drilling, is an important index for evaluating the wear resistance and self-sharpness of the core drill, as shown in Fig. 14. During the drilling of the first and second SiC_p/SiC composite micro-holes, the length reduction (ΔL) of the tool was 0.037 mm and 0.021 mm, respectively. At this stage, the tool is worn fast due to the brazing layer covering the top of the tool, preventing it from achieving normal machining performance. When drilling SiC_p/SiC composites, the brazing layer was worn off rapidly and the covered diamond grits were exposed, which were continuously worn. Therefore, the length reduction (ΔL) was higher during the initial two micro-hole drilling processes than subsequent micro-hole drilling. The high self-sharpness of the core drill maintains the length reduction at a low level, thus indicating slow wear and a long lifetime. After drilling two micro-holes of the SiC_p/SiC composite using the UVAD technique, the original wear period was passed, and the length reduction was approximately 0.01 mm for each drilling pass.

4 Results and discussion

4.1 Drilling force

The wear and self-sharpening behavior of the developed brazed diamond abrasive core drill was discussed in Section 3. In this section, the results of evaluating the machinability of the brazed diamond abrasive core drill by comparing it with that of the electroplated diamond core drill in UVAD are reported. When drilling with the electroplated diamond

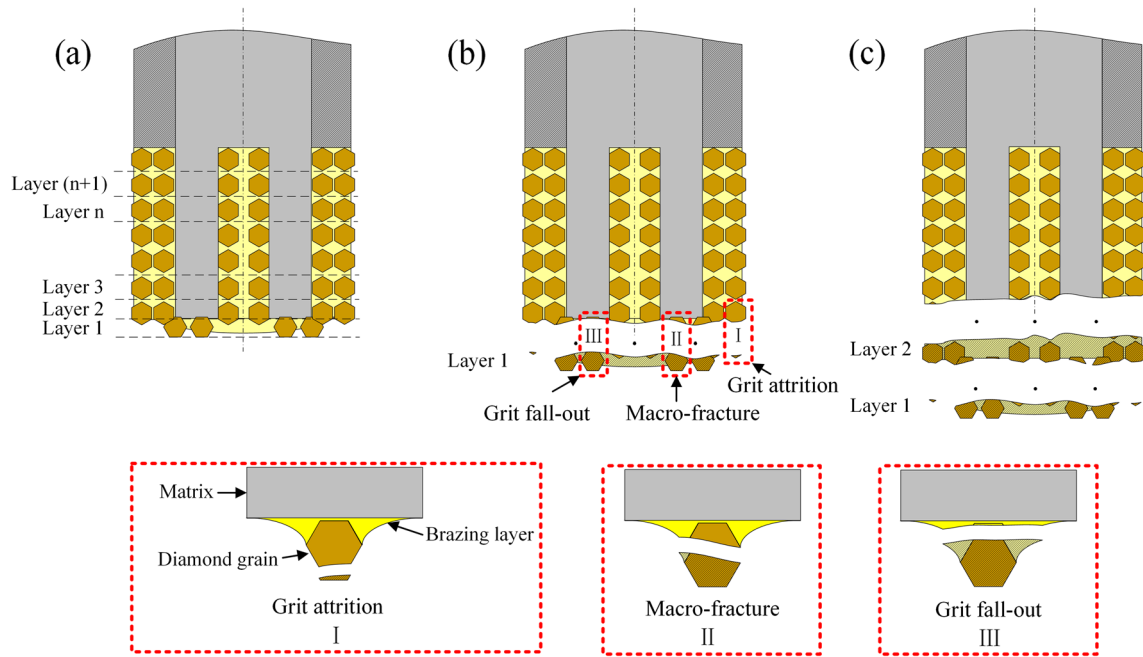


Fig. 13 Self-sharpness process of the brazed diamond abrasive core drill: **a** initial state of core drill, **b** wear process of core drill and **c** self-sharpness process of core drill

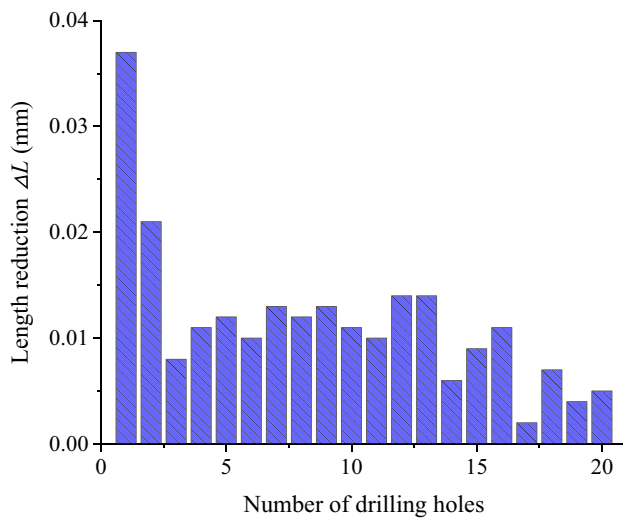


Fig. 14 Length reduction of the brazed diamond abrasive core drill

core drill, 12 micro-holes could be drilled in UVAD, and the average drilling forces increased slowly from 0.6 to 1.1 N, then increased significantly, and remained at approximately 2.5 N, as shown in Fig. 15. Ordinarily, tool cutting ability is always the key factor to restrict the drilling force. Therefore, the more severe the wear of the diamond grits, the greater the drilling force during the process. In addition, the actual working layer of electroplated diamond core drill is a single layer. Once the actual working layer of tool wear increases, the machinability of the core drill decreases, and the core

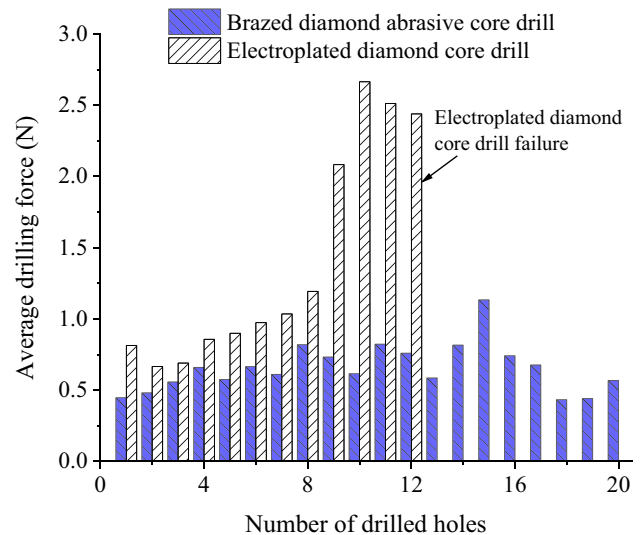


Fig. 15 Average drilling force

drill will eventually fail. The diamond grits were in the slow wear stage during the pre-drilling of SiC_r/SiC composites with electroplated diamond core drill (before 8 micro-holes), and the tool retained a specific cutting ability throughout the continuous drilling process. However, when drilling to the 9th hole, the diamond grits wore out seriously, and the cutting capacity of the tool rapidly declined. Then, when drilling to the 12th hole, the tool had completely worn out and was no longer functional.

With the novel brazed diamond abrasive core drill, 20 micro-holes could be machined using UVAD. In UVAD, the average drilling force was approximately 0.6 N, as shown in Fig. 15. The developed brazed diamond abrasive core drill could reduce the average drilling force by 76% compared with the electroplated diamond core drill. Additionally, the excellent self-sharpening capabilities of brazed diamond core drills, which keep the tool sharp throughout the drilling process and help to maintain the drilling force at a comparatively low level. In addition, the accuracy of the drilled hole diameter and the exit quality will be improved compared to the high drilling force because the lower drilling force will make the tool’s drilling process more stable.

4.2 Micro-hole diameter variation

The diameter of the SiC_p/SiC composite micro-holes is an important index for evaluating the machinability of core drills. The nominal diameter of a micro-hole is 1.4 mm. When using the electroplated diamond core drill in UVAD, the diameters of the ten micro-holes decreased from Φ 1.565 to Φ 1.395 mm and then increased to Φ 1.668 mm. The difference between the maximum and minimum diameters, Δ_{E-UVAD}, was 0.27 mm, as shown in Fig. 16. The decrease in diameter was due to the gradual wear of the core drill, loss of plating and matrix material, and grits at the corner, which decreased the diameter of the core drill, thereby decreasing the diameter of the micro-holes. With continued drilling of holes, the electroplated diamond core drill gradually wore out; the grits became blunt, and some fell out. The sharpness and machinability of the core drill deteriorated, the machining stability was poor, and severe vibration or chatter occurred during the drilling process, which increased the hole diameter.

With the developed brazed diamond abrasive core drill, the diameters of the 20 micro-holes in UVAD decreased gradually during the drilling process. The difference between the maximum and minimum diameters in UVAD, Δ_{B-UVAD}, was 0.03 mm. In addition, the diameter variation by using the developed brazed diamond abrasive core drill was smaller than that using the electroplated diamond core drill, as shown in Fig. 16. This indicates that the developed brazed diamond abrasive core drill has good self-sharpness and machinability during its lifetime and can restrict the diameter variation to a small level.

The dimensional accuracy of the electroplated diamond core drill and developed brazed diamond abrasive core drill shows different results, as shown in Fig. 16. Under the drilling process conditions investigated in this study, the electroplated diamond core drill exhibited fast wear rates,

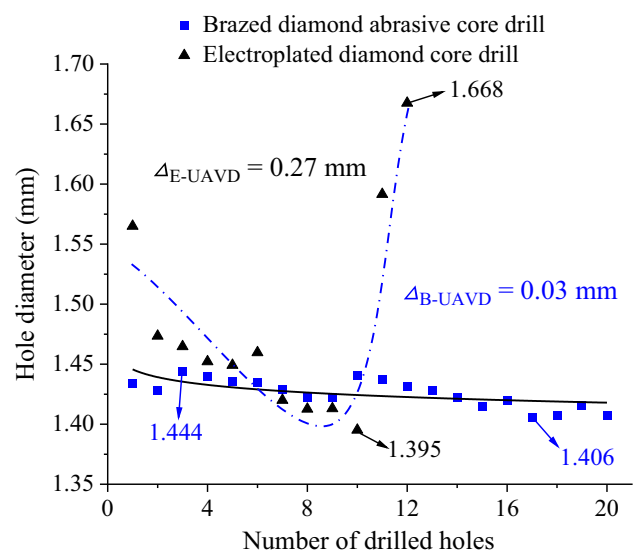


Fig. 16 Diameter of the SiC_p/SiC composite micro-holes

particularly on the diamond grits located on the side of the core drill. Therefore, the micro-hole diameter decreased rapidly in the drilling process, and the drilling dimensional accuracy was difficult to guarantee. On the contrary, the brazed diamond core drill had a longer working life than the electroplated diamond core drill while ensuring dimensional drilling accuracy because of its excellent self-sharpening ability and the role of the abrasive grits at the end of the tool working section in maintaining the hole diameter. In drilling 20 micro-holes, the hole diameter deviation was less than 0.03 mm, and the dimensional accuracy reached the IT9 level.

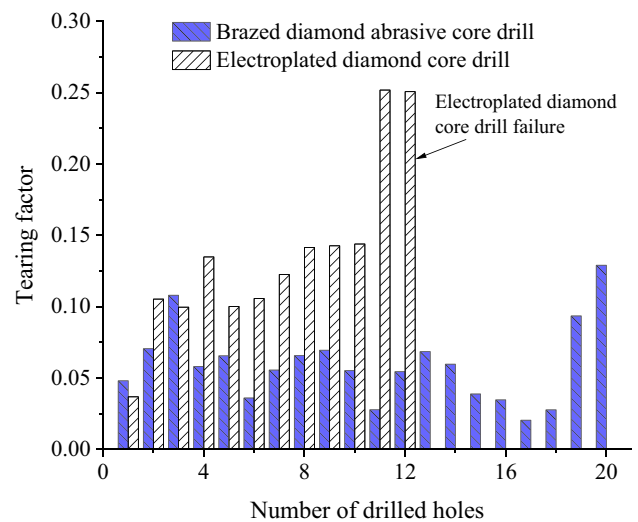


Fig. 17 Tearing factors of the micro-holes

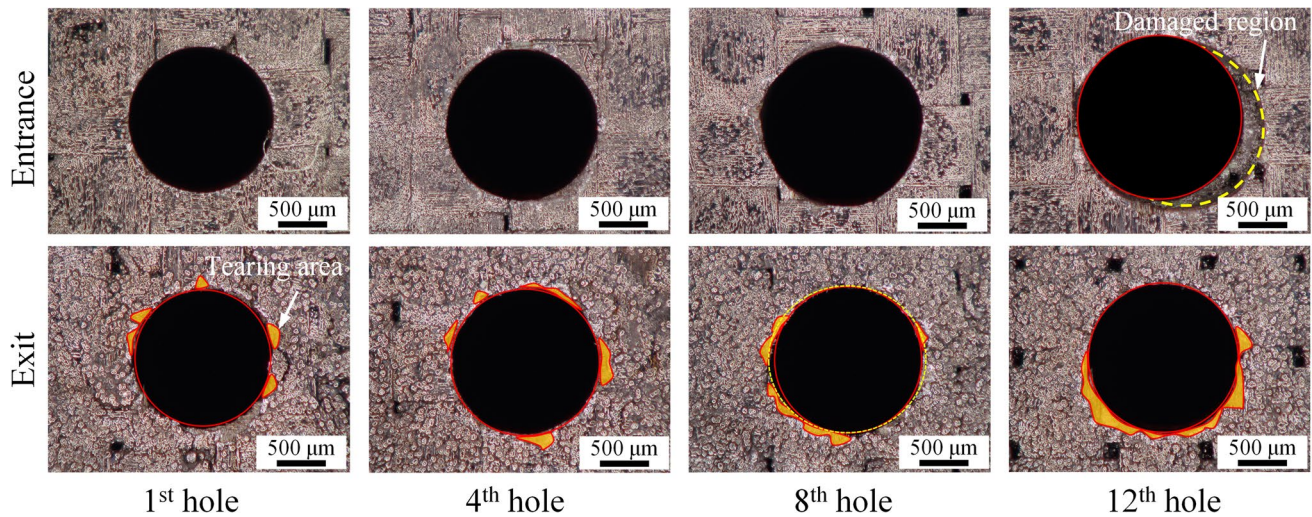


Fig. 18 Condition of entrance and exit of micro-holes machined by electroplated diamond core drill in UVAD

4.3 Hole surface quality

The exit tearing factor, which indicated the surface damage at the hole exit due to the electroplated diamond core drill, increased sharply with the drilling process and wear of the core drill, as shown in Fig. 17. In UVAD, the tearing factor increased from 0.04 to 0.15 when drilling ten micro-holes and then increased to 0.25 rapidly after drilling of 12 micro-holes. The entrance surface had hardly any tearing damage, whereas the exit of the holes had severe tearing damage, as shown in Fig. 18. In particular, when drilling the last two micro-holes, the sharpness and machinability of the core drill were poor, and the holes showed poor roundness. In addition, drilling was unstable at the last hole, and the core

drill exhibited vibration or chatter, leaving a damaged region at the entrance, as shown in Fig. 18.

When using the developed brazed diamond abrasive core drill, the tearing factor of the hole exit decreased as the drilling progressed; however, when drilling the last two micro-holes, the tearing factor increased owing to the poor machinability of the core drill (Fig. 17), which had reached the end of its lifetime. During UVAD, the tearing factor first decreased from 0.06 to 0.03 and then sharply increased to 0.14 for the last two holes, as shown in Fig. 17. Owing to the high sharpness of the brazed diamond abrasive core drill, the entrance of the micro-holes was of relatively good quality, whereas the exit exhibited some tearing damage. The exit tearing damage

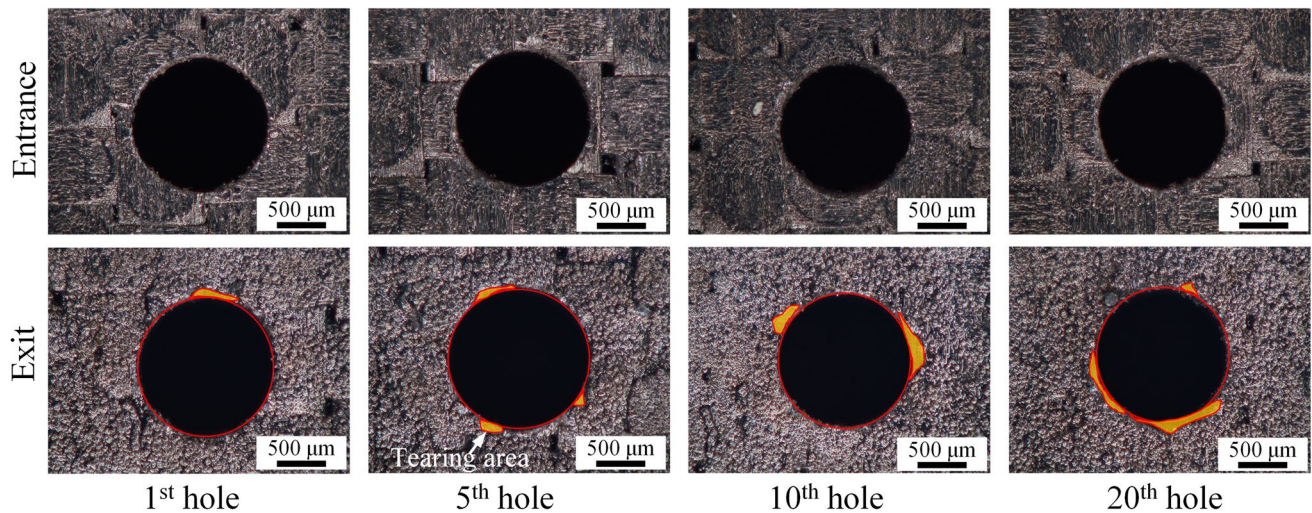


Fig. 19 Entrance and exit quality of micro-holes machined by brazed diamond abrasive core drill in UVAD

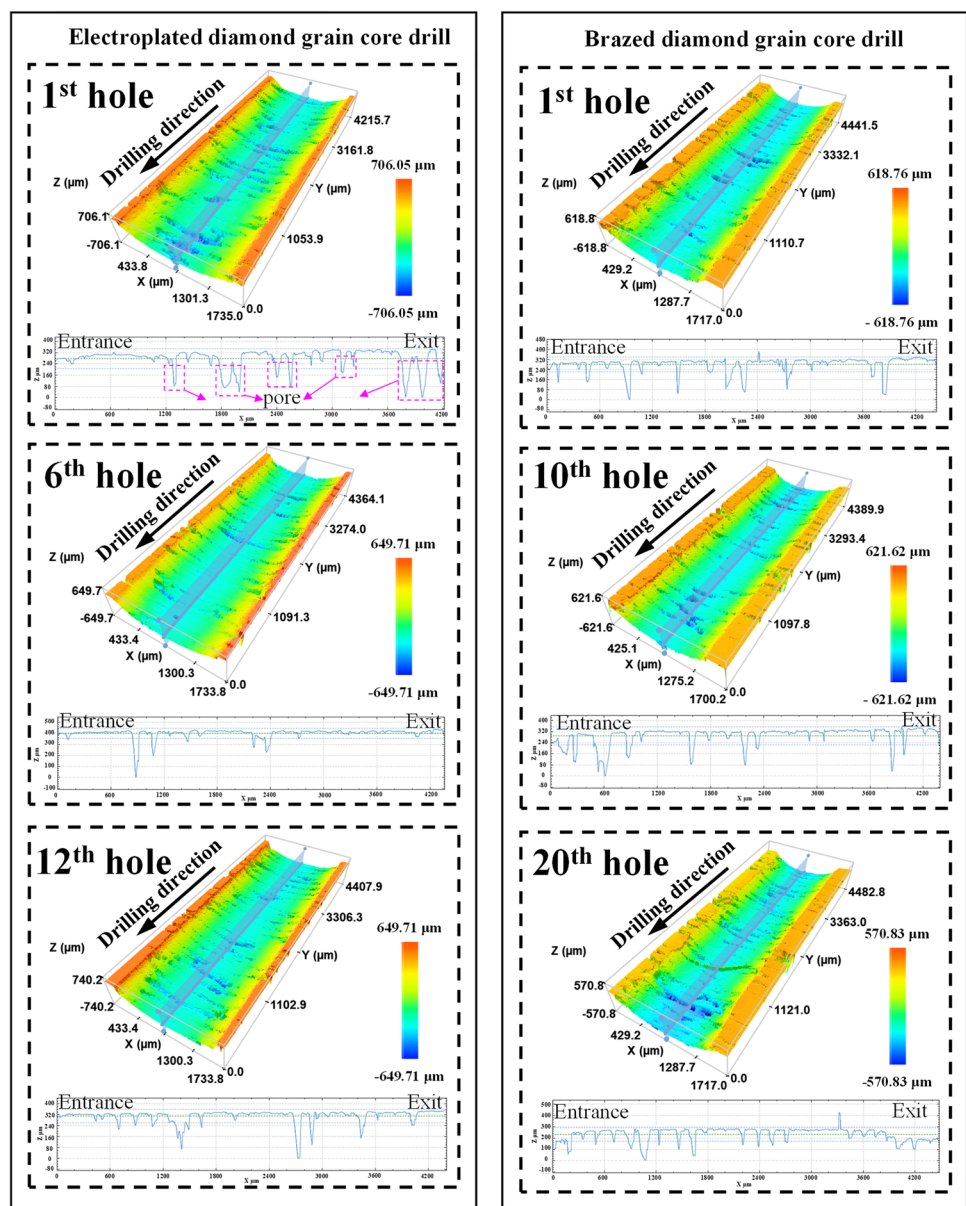
using the developed brazed diamond abrasive core drill was smaller than that of the electroplated diamond core drill, as shown in Figs. 18 and 19. Therefore, due to its high sharpness and machinability, the developed brazed diamond abrasive core drill demonstrated better drilling quality than the electroplated diamond core drill in UVAD.

4.4 The quality of the hole wall

The quality of the hole wall is one of the main concerns of the machining quality during the drilling process, and it is directly related to the functionality of the micro-hole. The factors affecting the quality of the hole wall are drilling

methods, parameters, and tool types. In this study, laser confocal microscopy was used to photograph and analyze the hole walls of different tools and different hole numbers, as shown in Fig. 20. The machined surface of the hole walls contained the pore structure of the material itself, and the surface formed by the SiC fiber yarn and the SiC ceramic matrix. Due to the porosity of 15–20% of the SiC_p/SiC composites, unevenly arranged concaves were distributed on the contour of the hole wall profile. According to the 3D morphology of the micro-hole wall drilled by electroplated diamond core drill and brazed diamond core drill, although the service life of the two tools was completely different, there were no significant differences in the morphology of the hole walls prepared by the two tools. It was because the

Fig. 20 3D morphology of drilled micro-hole walls



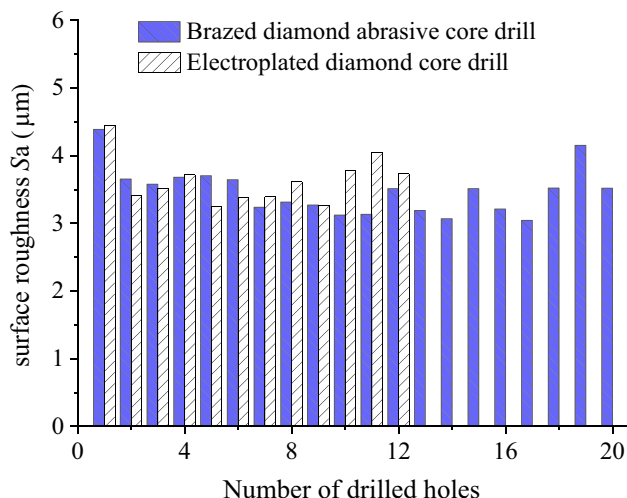


Fig. 21 Surface roughness of the hole walls

two tools used the same diamond grit size (120 mesh and average diameter of 100 µm), and the drilling method and parameters were the same. Therefore, the morphology of the hole walls formed during the drilling process was similar.

The surface roughness of the hole wall is an important evaluation index to evaluate the quality of the hole wall. Due to the anisotropic nature and fiber-woven structure of SiC_f/SiC composites, surface roughness S_a is a more accurate indicator for evaluating the machined surface quality of such materials. According to the width of the fiber yarns, the 3D cross-section of the hole wall with the area of 200 µm × 200 µm was intercepted to measure S_a as shown in Fig. 21. Under the condition of experimental parameters, the surface roughness S_a of all micro-holes was between S_a 3.25–4.45 µm and S_a 3.04–4.39 µm, respectively, by electroplated diamond core drill and brazed diamond core drill.

5 Conclusion

In this study, a novel brazed diamond abrasive core drill with high self-sharpness and excellent machinability was developed for drilling SiC_f/SiC composite micro-holes. The wear behavior and self-sharpness of the brazed diamond abrasive core drill were investigated. The drilling performance, including the drilling force, micro-hole diameter, and quality of the hole wall, was also evaluated by comparing it with that of the electroplated diamond core drill. The main conclusions are as follows:

- (1) The matrix of the core drill was machined with several grooves, and diamond grits were brazed in the grooves. During the drilling process, the grits become blunt and the machinability of the core drill degrades; in this case,

the brazing layer and matrix of the core drill, as well as the blunt grits, are reversibly removed by the hard and high-strength SiC_f/SiC composite. Then, the new and sharp grits in the grooves begin to protrude and again act to remove the workpiece material during drilling. This entails the self-sharpness process of the brazed diamond abrasive core drill, which maintains its good machinability

- (2) The proposed novel brazed diamond core drill exhibits grit attrition, macro-fracture, and fall-out of blunt grit during ultrasonic vibration-assisted drilling (UVAD) of SiC_f/SiC composite micro-holes. Owing to the higher wear resistance and self-sharpness, the proposed core drill has a longer lifetime, specifically 67% longer than those of the electroplated diamond core drill in UVAD, respectively. In addition, UVAD can further increase the dynamic sharpness of the core drill. The wear length of the proposed core drill is less than 0.02 mm after each UVAD of micro-holes
- (3) In the machining of SiC_f/SiC composite micro-holes, the proposed novel core drill achieves better drilling performance with UVAD. The drilling force can be decreased by up to 76%, and the micro-hole diameter difference can be reduced by 89% when compared with those of the electroplated diamond core drill. In addition, the proposed novel core drill can maintain the exit tearing factor below 0.15 in UVAD, whereas the electroplated diamond core drill can maintain the exit tear factor at only below 0.25. Besides, the hole wall surface roughness S_a of all micro-holes drilled by electroplated diamond core drill and brazed diamond core drill is similar, which are S_a 3.25–4.45 µm and S_a 3.04–4.39 µm, respectively.

In this study, Φ 1.4-mm micro-holes were successfully drilled in a SiC_f/SiC composite by using the developed novel brazed diamond abrasive core drill. The core drill showed advantages in its lifetime and drilling quality. Thus, this study provides fundamental guidance and basic data for the SiC_f/SiC composite machining industry. In the future, a smaller hole (e.g., Φ 0.7-mm micro-hole) will be drilled using the brazed diamond abrasive core drill with the same level of self-sharpness to further explore its machining ability.

Author contribution Jingyuan He and Ning Qian contributed to the conception of the study. Jingyuan He performed the experiments. Honghua Su, Wenfeng Ding, and Ning Qian contributed significantly to analysis and manuscript preparation. Jingyuan He performed the data analyses and wrote the manuscript. Yucan Fu and Jihua Xu helped perform the analysis with constructive discussions.

Funding The authors gratefully acknowledge the support of National Natural Science Foundation of China (Nos. 92060203 and 52205476), Science Center for Gas Turbine Project (No. P2022-AB-IV-002-001), and Outstanding Postdoctoral Program of Jiangsu Province (No. 2022ZB204).

Data availability The datasets used or analyzed during the current study are available from the corresponding author on reasonable request.

Code availability This is not applicable.

Declarations

Ethics approval The article follows the guidelines of the Committee on Publication Ethics (COPE) and involves no studies on human or animal subjects.

Consent to participate This is not applicable.

Consent for publication This is not applicable.

Competing interests The authors declare no competing interests.

References

- Li HH, Yuan XY, Zhao PH, Ping ZY, Liu Y, Guo SW (2023) A synergistic strategy for SiC/C nanofibers@MXene with core-sheath microstructure toward efficient electromagnetic wave absorption and photothermal conversion. *Appl Surf Sci* 613:155998. <https://doi.org/10.1016/j.apsusc.2022.155998>
- Lü XX, Li LB, Sun JJ, Yang JH, Jiao J (2022) Microstructure and tensile behavior of (BN/SiC)_n coated SiC fibers and SiC/SiC minicomposites. *J Eur Ceram Soc* 43(5):1828–1842. <https://doi.org/10.1016/j.jeurceramsoc.2022.12.032>
- Zhang XH, Gao HS, Wen ZX, Li MY, Zhou XG, Yue ZF (2020) Effect of film cooling holes on the mechanical properties of 3D braided SiC_p/SiC composites at 1350°C in air. *Ceram Int* 46(6):7982–7990. <https://doi.org/10.1016/j.ceramint.2019.12.020>
- Wang X, Ding WF, Zhao B (2022) A review on machining technology of aero-engine casings. *J Adv Manuf Sci Technol* 2(3):2022011–2022011. <https://doi.org/10.51393/j.jamst.2022011>
- An QL, Chen J, Ming WW, Chen M (2021) Machining of SiC ceramic matrix composites: a review. *Chin J Aeronaut* 34(4):540–567. <https://doi.org/10.1016/j.cja.2020.08.001>
- Wang F, Luo JJ, Li M, Deng Y (2014) A study on the technical method of drilling micro holes on new CMC-SiC with femtosecond laser. *Appl Mech Mater* 543–547:3924–3930. <https://doi.org/10.4028/www.scientific.net/AMM.543-547.3924>
- Zhang J, Liu RJ, Jian YJ, Wan F, Wang YF (2022) Degradation mechanism of SiC_p/SiC composites after long-time water vapor and oxygen corrosion at 1300°C. *Corros Sci* 197:110099. <https://doi.org/10.1016/j.corsci.2022.110099>
- Wang D, Cao HR (2022) A comprehensive review on crack modeling and detection methods of aero-engine disks. *J Adv Manuf Sci Technol* 2(3):2022012–2022012. <https://doi.org/10.51393/j.jamst.2022012>
- Zeng JH, Zhang QL, Zhao J, Cai YB, Chu CL, Zhu YD, Xu JH (2022) The formed surface characteristics of SiC_p/SiC composite in the nanosecond pulsed laser ablation. *Ceram Int* 48(24):36860–36870. <https://doi.org/10.1016/j.ceramint.2022.08.251>
- Huang B, Wang WH, Jiang RS, Xiong YF, Liu C (2022) Experimental study on ultrasonic vibration-assisted drilling micro-hole of SiC_p/SiC ceramic matrix composites. *Int J Adv Manuf Technol* 120:8031–8044. <https://doi.org/10.1007/s00170-022-09186-0>
- Hasan M, Zhao JW, Jiang ZY (2017) A review of modern advancements in micro drilling techniques. *J Manuf Process* 29:343–375. <https://doi.org/10.1016/j.jmapro.2017.08.006>
- Chen J, An QL, Ming WW, Chen M (2019) Hole exit quality and machined surface integrity of 2D C_p/SiC composites drilled by PCD tools. *J Eur Ceram Soc* 39(14):4000–4010. <https://doi.org/10.1016/j.jeurceramsoc.2019.05.057>
- Wang J, Zhang YH, Liu YS, Fang H, Cao LY, Dong N, Luo R, Cheng GH, Cao YJ, Zhang Q (2023) Effect of SiC/SiC composites density on nanosecond-laser machining behaviors. *Ceram Int* 49(3):5199–5208. <https://doi.org/10.1016/j.ceramint.2022.10.038>
- Li WN, Zhang RH, Liu YS, Wang CH, Wang J, Yang XJ, Cheng LF (2016) Effect of different parameters on machining of SiC/SiC composites via pico-second laser. *Appl Surf Sci* 364:378–387. <https://doi.org/10.1016/j.apsusc.2015.12.089>
- Chen J, An QL, Gong QH, Zeng DB, Chen M (2022) Machinability improvement in milling of SiC_p/SiC composites based on laser controllable ablation pretreatment. *J Eur Ceram Soc* 43(4):1352–1365. <https://doi.org/10.1016/j.jeurceramsoc.2022.11.070>
- Kumar SS, Thrinadh J, Datta S (2021) Parametric studies on SiC-abrasive jet assisted machining of alumina ceramics. *Mater Today Proc* 44:1643–1652. <https://doi.org/10.1016/j.matpr.2020.11.823>
- Zhang YF, Liu D, Zhang WJ, Zhu HT, Huang CZ (2022) Hole characteristics and surface damage formation mechanisms of C_p/SiC composites machined by abrasive waterjet. *Ceram Int* 48(4):5488–5498. <https://doi.org/10.1016/j.ceramint.2021.11.093>
- Zhang YB, Li WY, Tang LZ, Li CH, Liang XL, Xu SQ, Zafar S, Shubham S, Chen Y, Liu B, Zhou ZM (2023) Abrasive water jet tool passivation: from mechanism to application. *J Adv Manuf Sci Technol* 3(1):2022018–2022018. <https://doi.org/10.51393/j.jamst.2022018>
- Dong XY, Shin YC (2017) Improved machinability of SiC/SiC ceramic matrix composite via laser-assisted micromachining. *Int J Adv Manuf Technol* 90:731–739. <https://doi.org/10.1007/s00170-016-9415-5>
- Zhai ZY, Wang WJ, Mei XS, Li M, Cui JL, Wang FC, Pan AF (2018) Effect of the surface microstructure ablated by femtosecond laser on the bonding strength of EBCs for SiC/SiC composites. *Opt Commun* 424:137–144. <https://doi.org/10.1016/j.optcom.2018.04.055>
- Zhang RH, Li WN, Liu YS, Wang CH, Wang J, Yang XJ, Cheng LF (2015) Machining parameter optimization of C/SiC composites using high power picosecond laser. *Appl Surf Sci* 330:321–331. <https://doi.org/10.1016/j.apsusc.2015.01.010>
- Liu C, Zhang XZ, Gao L, Jiang XG, Li C, Yang T (2021) Feasibility of micro-hole machining in fiber laser trepan drilling of 2.5D C_f/SiC composite: experimental investigation and optimization. *Optik (Stuttg)* 242:167186. <https://doi.org/10.1016/j.ijleo.2021.167186>
- Detwiler KN, Opila EJ (2022) Oxidation of SiC/BN/SiC ceramic matrix composites in dry and wet oxygen at intermediate temperatures. *J Eur Ceram Soc* 42(10):4110–4120. <https://doi.org/10.1016/j.jeurceramsoc.2022.04.003>
- Sheikh-Ahmad JY (2016) Hole quality and damage in drilling carbon/epoxy composites by electrical discharge machining. *Mater Manuf Process* 31:941–950. <https://doi.org/10.1080/10426914.2015.1048368>
- Wei CJ, Zhao L, Hu DJ, Ni J (2013) Electrical discharge machining of ceramic matrix composites with ceramic fiber reinforcements. *Int J Adv Manuf Technol* 64:187–194. <https://doi.org/10.1007/s00170-012-3995-5>
- Hrechuk A, Bushlya V, M'Saoubi R, Ståhl JE (2018) Experimental investigations into tool wear of drilling CFRP. *Procedia Manuf* 25:294–301. <https://doi.org/10.1016/j.promfg.2018.06.086>
- Li PN, Qiu XY, Li CP, Niu QL, Chen AH, Ko TJ (2019) Hole exit damage and tool wear during the drilling of CFRP with a double-point angle drill. *J Mech Sci Technol* 33:2363–2370. <https://doi.org/10.1007/s12206-019-0436-5>
- Zhang BY, Sui TY, Lin B, Zheng W, Li SP, Fang S, Huang Y, Feng YQ (2022) Drilling process of C_p/SiC ceramic matrix composites: cutting force modeling, machining quality and PCD tool

- wear analysis. *J Mater Process Technol* 304:117566. <https://doi.org/10.1016/j.jmatprotec.2022.117566>
29. Zou F, Chen J, An QL, Cai XJ, Chen M (2020) Influences of clearance angle and point angle on drilling performance of 2D C_p/SiC composites using polycrystalline diamond tools. *Ceram Int* 46(4):4371–4380. <https://doi.org/10.1016/j.ceramint.2019.10.161>
 30. Wang X, Popov VL, Yu ZJ, Li YQ, Xu JK, Li Q, Yu HD (2022) Evaluation of the cutting performance of micro-groove-textured PCD tool on SiCp/Al composites. *Ceram Int* 48(21):32389–32398. <https://doi.org/10.1016/j.ceramint.2022.07.182>
 31. Ding K, Fu YC, Su HH, Chen Y, Yu XZ, Ding GZ (2014) Experimental studies on drilling tool load and machining quality of C/SiC composites in rotary ultrasonic machining. *J Mater Process Technol* 214(12):2900–2907. <https://doi.org/10.1016/j.jmatprotec.2014.06.015>
 32. He JY, Su HH, Qian N, Xu PF (2022) Machining performance analysis of rotary ultrasonic-assisted drilling of SiC_p/SiC composites. *Crystals* 12(11):1658. <https://doi.org/10.3390/cryst12111658>
 33. Wang JJ, Feng PF, Zheng JZ, Zhang JF (2016) Improving hole exit quality in rotary ultrasonic machining of ceramic matrix composites using a compound step-taper drill. *Ceram Int* 42(12):13387–13394. <https://doi.org/10.1016/j.ceramint.2016.05.095>
 34. Tawakoli T, Azarhoushang B (2011) Intermittent grinding of ceramic matrix composites (CMCs) utilizing a developed segmented wheel. *Int J Mach Tools Manuf* 51(2):112–119. <https://doi.org/10.1016/j.ijmactools.2010.11.002>
 35. Xue F, Zheng K, Liao WH, Shu J, Miao DD (2021) Experimental investigation on fatigue property at room temperature of C/SiC composites machined by rotary ultrasonic milling. *J Eur Ceram Soc* 41(6):3341–3356. <https://doi.org/10.1016/j.jeurceramsoc.2021.01.046>
 36. Feng PF, Wang JJ, Zhang JF, Zheng JZ (2017) Drilling induced tearing defects in rotary ultrasonic machining of C/SiC composites. *Ceram Int* 43(1):791–799. <https://doi.org/10.1016/j.ceramint.2016.10.010>
 37. Li Z, Yuan SM, Ma J, Shen J, Batako ADL (2022) Cutting force and specific energy for rotary ultrasonic drilling based on kinematics analysis of vibration effectiveness. *Chin J Aeronaut* 35(1):376–387. <https://doi.org/10.1016/j.cja.2020.12.023>
 38. Wu BF, Zhao B, Ding WF, Su HH (2021) Investigation of the wear characteristics of microcrystal alumina abrasive wheels during the ultrasonic vibration-assisted grinding of PTMCs. *Wear* 477:203844. <https://doi.org/10.1016/j.wear.2021.203844>
 39. Sonia P, Jain JK, Saxena KK (2021) Influence of ultrasonic vibration assistance in manufacturing processes: a review. *Mater Manuf Process* 36:1451–1475. <https://doi.org/10.1080/10426914.2021.1914843>
 40. Su QT, Li XD, Lu Y, Huang S (2022) Designing an ultrasonic array device to transport space particle suspension. *J Adv Manuf Sci Technol* 2(1):2022004–2022004. <https://doi.org/10.51393/j.jamst.2022004>
 41. Wang MX, Yu HD, Xu JK, Chen GJ, Dai B, Wang S (2021) Amplitude effect on micro-hole drilling of 3D needled C_p/SiC by ultrasonic vibration. *Ceram Int* 47(24):34987–35001. <https://doi.org/10.1016/j.ceramint.2021.09.040>
 42. Yang YK, Zheng K, Dong S, Sun LJ, Sun ZW (2023) Investigation into temperature and its effects on hole wall quality in rotary ultrasonic countersinking of thin-walled CFRP/Al stacks. *J Adv Manuf Sci Technol* 3(2):2023002–2023002. <https://doi.org/10.51393/j.jamst.2023002>
 43. Ding K, Li QL, Lei WN, Zhang CD, Xu MZ, Wang X (2022) Design of a defined grain distribution brazed diamond grinding wheel for ultrasonic assisted grinding and experimental verification. *Ultrasonics* 118:106577. <https://doi.org/10.1016/j.ultras.2021.106577>
 44. Zou ZC, He L, Zhou T, Zhang WQ, Tian PF, Zhou XR (2023) Research on inverse identification of Johnson-Cook constitutive parameters for turning 304 stainless steel based on coupling simulation. *J Mater Res Technol* 23:2244–2262. <https://doi.org/10.1016/j.jmrt.2023.01.090>

Publisher's note Springer Nature remains neutral with regard to jurisdictional claims in published maps and institutional affiliations.

Springer Nature or its licensor (e.g. a society or other partner) holds exclusive rights to this article under a publishing agreement with the author(s) or other rightsholder(s); author self-archiving of the accepted manuscript version of this article is solely governed by the terms of such publishing agreement and applicable law.